



Cell-sized mechanosensitive and biosensing compartment programmed with DNA†

Sagardip Majumder,^{‡,a} Jonathan Garamella,^{‡,b} Ying-Lin Wang,^c Maxwell DeNies,^d Vincent Noireaux^{*b} and Allen P. Liu^{ib,*adef}

Cite this: *Chem. Commun.*, 2017, 53, 7349

Received 4th May 2017,
Accepted 12th May 2017

DOI: 10.1039/c7cc03455e

rsc.li/chemcomm

The bottom-up construction of cell-sized compartments programmed with DNA that are capable of sensing the chemical and physical environment remains challenging in synthetic cell engineering. Here, we construct mechanosensitive liposomes with biosensing capability by expressing the *E. coli* channel MscL and a calcium biosensor using cell-free expression.

Cell-free expression (CFE) has been recently reshaped into a highly versatile technology applicable to an increasing number of research areas.¹ The new generation of DNA-dependent cell-free transcription–translation systems (TXTL) has been engineered to address applications over a broad spectrum of engineering and fundamental disciplines, from synthetic biology to biophysics and chemistry.^{2–4} Modern TXTL platforms are used for medicine and biomolecular manufacturing, such as the production of vaccine and therapeutics.^{5,6} By performing non-natural chemistries,^{3,7,8} the TXTL technology has been improved to expand the molecular repertoire of biological systems. Because the time for design–build–test cycle is dramatically reduced, TXTL has become a powerful platform to rapidly prototype genetic programs *in vitro*, from testing single regulatory elements to recapitulating metabolic pathways.⁹ Remarkably, the new TXTL systems have also been prepared so as to work at many different scales and in different experimental settings. As such, TXTL reactions can be carried out in volumes spanning more than twelve

orders of magnitudes, from bulk reactions to microfluidics and artificial cell systems.^{2,10–13}

The bottom-up construction of synthetic cells that recapitulates gene expression has become an effective means to characterize biological functions in isolation and to prototype cell-sized compartments as chemical bioreactors for applications in biotechnology.^{14,15} In particular, engineering artificial cells integrating active membrane functions is critical to develop mechanically robust compartments capable of sensing the physical and chemical environment. Such undertaking, however, remains challenging as only a few synthetic cell systems loaded with executable genetic information and harboring membrane sensors have been achieved.¹⁶ In this work, we construct synthetic cells capable of responding to osmotic pressure by expressing the *E. coli* mechanosensitive membrane protein MscL using a TXTL system encapsulated into synthetic liposomes. Using the calcium sensitive reporter G-GECO, we demonstrate that the osmotic pressure and calcium intake can be detected simultaneously, at different concentrations of the divalent ion. TXTL is carried out with a highly versatile all *E. coli* cell-free toolbox based on the endogenous transcription machinery (*E. coli* core RNA polymerase and sigma factor 70, $\sigma 70$). We characterize the channel function by monitoring the fluorescence of G-GECO and the leak of polymers of various sizes. Our novel approach expands the functional capabilities of encapsulated cell-free TXTL reactions and demonstrates, for the first time, that synthetic cell systems with biosensing interfaces can be achieved by directly expressing membrane proteins inside liposomes.

Our general methodology is to encapsulate TXTL reactions within phospholipid vesicles as a versatile platform that recapitulates *in vitro* transcription–translation for producing proteins that endow biosensing and molecular transport properties to the vesicles (Fig. 1A). DNA-based cell-free protein synthesis inside liposomes links the information contained in the DNA to the phenotype of synthetic cells in a reduced environment suitable for isolation and characterization of cellular functions. Like a complex chemical reaction that can be broken down to elementary processes, biochemical reactions based on genetic circuits can also be constructed to control rates of protein production. Such settings are conveniently

^a Department of Mechanical Engineering, University of Michigan, Ann Arbor, Michigan, USA. E-mail: allenliu@umich.edu

^b Department of Physics and Astronomy, University of Minnesota, Minneapolis, Minnesota, USA. E-mail: noireaux@umn.edu

^c Department of Biomedical Engineering, National Cheng Kung University, Tainan, Taiwan

^d Cellular and Molecular Biology Program, University of Michigan, Ann Arbor, Michigan, USA

^e Department of Biomedical Engineering, University of Michigan, Ann Arbor, Michigan, USA

^f Biophysics Program, University of Michigan, Ann Arbor, Michigan, USA

† Electronic supplementary information (ESI) available: Materials and methods and supplementary figures. See DOI: 10.1039/c7cc03455e

‡ S. M. and J. G. contributed equally to this work.

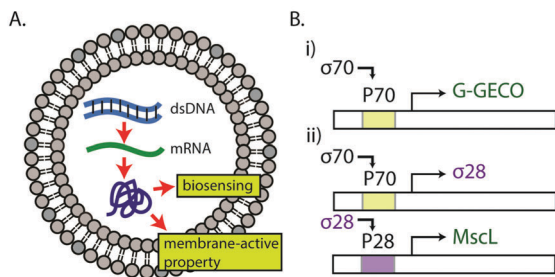


Fig. 1 Schematics of protein synthesis in liposomes and gene circuits. (A) dsDNA is transcribed into mRNA, which is then translated to a biosensing fluorescent reporter protein (G-GECO) and a mechanosensitive membrane-active protein (MscL). (B) Gene circuits used in this work. (i) The *E. coli* housekeeping transcription factor sigma 70 activates the promoter P70a. (ii) The sigma 28 cascade requires the expression of sigma 28 protein, expressed through the P70a promoter. The sigma 28 transcription factor activates the corresponding promoter P28a.

adjusted in TXTL by either choosing the appropriate plasmids stoichiometry and circuit architectures, or by calibrating the strength of promoters and ribosome binding sites.² In this work, we used two different genetic circuit schemes to produce proteins of interests (Fig. 1B). In the first scheme, the endogenous *E. coli* core RNA polymerase $\sigma 70$ drives the transcription of downstream coding sequence through the constitutive promoter P70a.² Our second scheme is a transcriptional activation cascade where P70a/ $\sigma 70$ drives the expression of sigma factor 28 ($\sigma 28$) that is required for subsequent expression from a P28a promoter sequence specific to $\sigma 28$. We first used the reporter protein deGFP to characterize the circuit functions and features.² deGFP is a slightly modified version of eGFP with identical fluorescence properties. Both schemes were then used to express G-GECO, a genetically encoded green fluorescence protein whose fluorescence depends on calcium concentration,¹⁷ and the *E. coli* mechanosensitive channel of large conductance (MscL) for biosensing and incorporating a membrane-active property, respectively.

We first performed bulk reactions (10 μ l reactions) and compared deGFP expression kinetics of the single-step circuit vs. the transcriptional activation cascade circuit. As expected, the requirement for $\sigma 28$ to drive expression of deGFP in the transcriptional activation resulted in a delay in deGFP expression compared to the single-step circuit (Fig. 2A). The delay observed for the cascade, on the order of 15 minutes, corresponded to the amount of time necessary for the synthesis of $\sigma 28$. The bulk reaction persisted for many hours and deGFP production began to slow down after 8 hours and reached a plateau after 10 hours. The time course observed in these experiments is typical for TXTL reactions where protein synthesis ceases due to resource limitation (depletion of nucleotides and amino acids), change in the biochemical environment (pH) and accumulation of reaction byproducts. We next asked whether compartmentalization could preserve the delay in deGFP production that we observed in the bulk reactions. Using a single-step emulsion approach by vortexing aqueous TXTL reactions in 2% Span 80 dissolved in mineral oil, we produced emulsion droplets with a wide range of sizes encapsulating the TXTL reactions. As clearly evident, we observed deGFP expression as early as

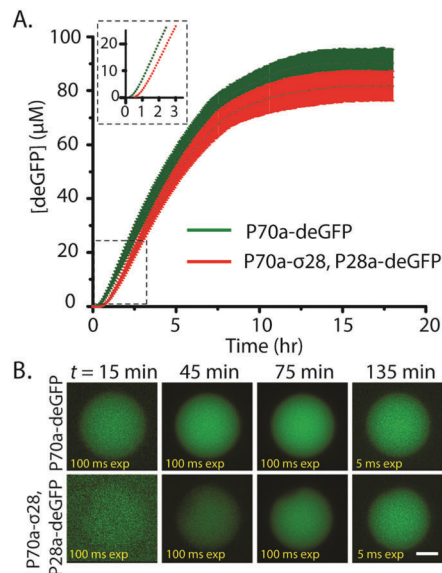


Fig. 2 deGFP synthesis in bulk reactions, single emulsions, and liposomes. (A) Kinetics of expression. Plasmid P70a-deGFP fixed at 5 nM, P70a-S28 fixed at 0.2 nM, and P28a-deGFP fixed at 5 nM. Inset: 0–3 hours magnified. (B) deGFP synthesis in liposomes using both the P70a plasmid and P28a cascade. Scale bar: 5 μ m.

45 minutes for the single-step circuit compared to relatively weak fluorescence after 1 hour for the transcriptional activation cascade (Fig. S1, ESI[†]). Fluorescence intensity reached maximum after ~ 2 hours in both cases. The shorter protein production time in single emulsions is consistent with a faster rate of resource depletion in a compartmentalized system as compared to a bulk system,¹⁰ as well as to the limited supply of oxygen necessary for cell-free TXTL. We next created synthetic cells by encapsulating TXTL reactions into phospholipid vesicles that have a physical boundary comparable to real living cells. We used a reverse emulsion technique for generating liposomes² and we accounted for the delay in imaging start time due to preparation (estimated to be ~ 15 min). Because of the initial low protein production in vesicles, we acquired images at a high exposure time during the first hour (100 ms compared to 5 ms after 75 minutes of incubation) so that some fluorescence signals were observable at the earlier time points. Consistent with the experiments carried out under bulk conditions and in single emulsions, there was a clear delay in deGFP production in the transcriptional activation cascade (Fig. 2B). deGFP production leveled off after ~ 10 hours. The longer lasting expression compared to single emulsion is likely due to the availability of oxygen from the outer aqueous solution. Together, these experiments demonstrate that a cascaded circuit can delay reporter expression and that we can achieve robust protein expression by compartmentalizing CFE reactions.

Phospholipid vesicles are particularly useful for encapsulating TXTL reaction in cell-sized compartments because lipidic bilayers are the natural substrates for membrane proteins such as channels and receptors. Expressing membrane proteins is a critical step towards constructing synthetic cells with functional interfaces to provide, for instance, transport or catalytic capabilities to a vesicle. In this regard, only a few of such artificial systems with membrane

protein channels and sensors have been achieved so far.^{11,16} As a model system, we expressed MscL using the cascaded transcriptional activation circuit. MscL is a bacterial membrane protein that senses an increase in membrane tension and opens a pore of ~ 2.5 nm diameter to allow influx/efflux of molecules down the concentration gradient. It is thought to serve as the emergency release valve during osmotic downshock without which bacteria can lyse due to elevated osmotic pressure. We and others have shown that an increase in osmotic pressure or membrane tension can directly gate MscL.^{18–20} Integrating active MscL into the membrane of synthetic cells by CFE is important for several reasons. First, it provides increased mechanical robustness to the vesicles against bursting by equilibrating osmotic pressure. It is a necessary step towards constructing synthetic cells robust enough to be used outside laboratory conditions. Second, the channel diameter is ideal to pass small nutrients molecules and feed the synthetic cells, while keeping the TXTL machineries inside. Third, it demonstrates that TXTL supports the expression of mechanosensitive membrane proteins that could be used as a means to test MscL mutants in the future. When expressing MscL using the transcriptional activation cascade, the delay in MscL expression (about 15 minutes) is advantageous because it corresponds to the amount of time needed to prepare the liposomes. We first expressed MscL-eGFP to visualize MscL localization. We observed the accumulation of MscL-eGFP at the membrane over time as expected (Fig. S2, ESI[†]). In order to test MscL function, we developed a simple dye-leakage assay where TRITC-labeled dextrans of different molecular weight (3, 10, and 70 kDa) and TXTL reaction producing wild type MscL were co-encapsulated using the emulsion method to make liposomes (Fig. 3A). We expressed the native MscL without a fluorescent protein tag as MscL fusion proteins have a higher activation tension threshold.¹⁸ In our experiments, we relied on the osmotic pressure from a hypo-osmotic feeding solution (~ 630 mOsm) relative to the encapsulated TXTL reaction (~ 700 mOsm). In the absence of MscL expression, 5 μ M of 3000 Da TRITC-dextran remained encapsulated in the vesicle after 2 hours (Fig. 3B). In contrast, MscL expression led to dye-leakage after 20–30 minutes. When a larger 10 000 Da TRITC-dextran was used, we observed complete dye-leakage after 60 minutes in MscL-expressing vesicles (Fig. S3A and B, ESI[†]). Larger dextran molecules at 70 000 Da were completely retained after 120 minutes with or without MscL expression (Fig. S3C, ESI[†]), with no leakage observed after 12 hours of incubation (data not shown). We also tested the leakage of two proteins, deGFP (27 kDa) and BSA-TRITC (60 kDa). Both were also completely retained inside the liposomes in MscL-expressing vesicles after 2 hours of incubation (Fig. S3D, ESI[†]). No leakage was observed after overnight incubation (data not shown).

Our next challenge was to use a genetically-encoded reporter and demonstrate that we can couple a mechanical input to biosensing. We cloned the genetically-encoded calcium ion (Ca^{2+}) biosensor G-GECO that is composed of a circularly permuted GFP fused to the calmodulin (CaM)-binding region of myosin light chain kinase M13 at its N-terminus and CaM at its C-terminus.²¹ G-GECO is dim in the absence of Ca^{2+} and bright when bound to Ca^{2+} with a Ca^{2+} -dependent fluorescence increase of ~ 23 – 26 fold (Fig. 4A).⁷ We cloned G-GECO under the P70a promoter and verified that it can

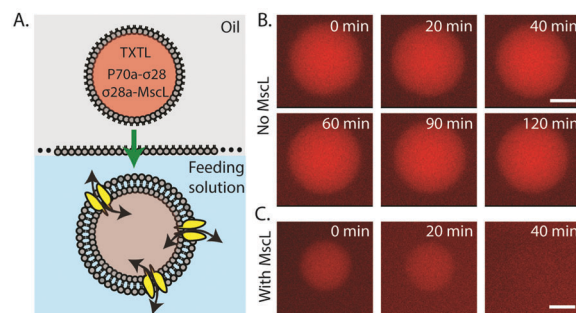


Fig. 3 Leakage of a 3 kDa TRITC-dextran in liposomes in the absence or presence of MscL. (A) Schematic of the encapsulation of a cell-free reaction containing 3 kDa TRITC-dextran (5 μ M), P70a-S28 (0.2 nM), and P28a-MscL (5 nM) into liposomes via the water-in-oil emulsion transfer method. (B) Fluorescence images of liposomes containing 3 kDa TRITC-dextran over a 2 hour period with only P70a-S28 added to the cell-free reaction. (C) Fluorescence images of liposomes containing 3 kDa TRITC-dextran over a 40 minute period with P70a-S28 and P28a-MscL added to the cell-free reaction. Scale bar: 5 μ m.

sense Ca^{2+} in a plate reader assay (Fig. S4A, ESI[†]). To eliminate traces of Ca^{2+} present in TXTL reactions estimated to be up to 1 mM Ca^{2+} , we added 1 mM EGTA to the TXTL reactions so that G-GECO can report an increase in calcium level when externally added to the reactions. Both G-GECO and MscL-eGFP can be produced together in a single TXTL reaction, as shown by the increased fluorescence level by G-GECO after adding 1 mM Ca^{2+} at 120 minutes after TXTL started (Fig. S4B, ESI[†]).

To create mechanosensitive-biosensing vesicles, we employed double emulsion templated vesicles generated by droplet microfluidics.^{22,23} We have previously used this approach and showed that small molecules from the feeding solution can enter encapsulated vesicles containing integrated synthesis, assembly, and translation (iSAT) reactions.¹⁰ We have also shown that Ca^{2+} can enter a double emulsion droplet with an ultrathin oil layer as the middle phase when the droplet is under hypo-osmotic shock.²⁴ However, Ca^{2+} as a charged ion cannot cross a lipid bilayer. When G-GECO was expressed in the presence of 1.5 mM Ca^{2+} inside a vesicle, fluorescence was readily detected after 90 minutes, demonstrating that G-GECO can be used to detect increased calcium concentration in an artificial cell (Fig. 4B). As expected, if Ca^{2+} is added to the outside (at 10 mM) of G-GECO expressing vesicle, no G-GECO fluorescence was observed because Ca^{2+} is impermeable to phospholipid membrane (Fig. S5A, ESI[†]). However, addition of a calcium ionophore A23187 allowed rapid entry of Ca^{2+} and G-GECO fluorescence was readily observed in as little as 10 minute post A23187 addition (Fig. S5B, ESI[†]).

To couple mechanical input to sensing the external environment, we co-expressed G-GECO (under P70a promoter) and MscL (under P28a promoter) in TXTL for 2 or 3 hours and then encapsulated the reaction into double emulsion templated vesicles. Under iso-osmotic condition, we did not observe G-GECO fluorescence for over 10 hours, our longest observation time point (Fig. 4C(i)). In contrast, hypo-osmotic condition of ~ 100 mOsm osmotic difference between inside and outside the vesicle robustly led to an increase in G-GECO fluorescence as Ca^{2+} was able to enter

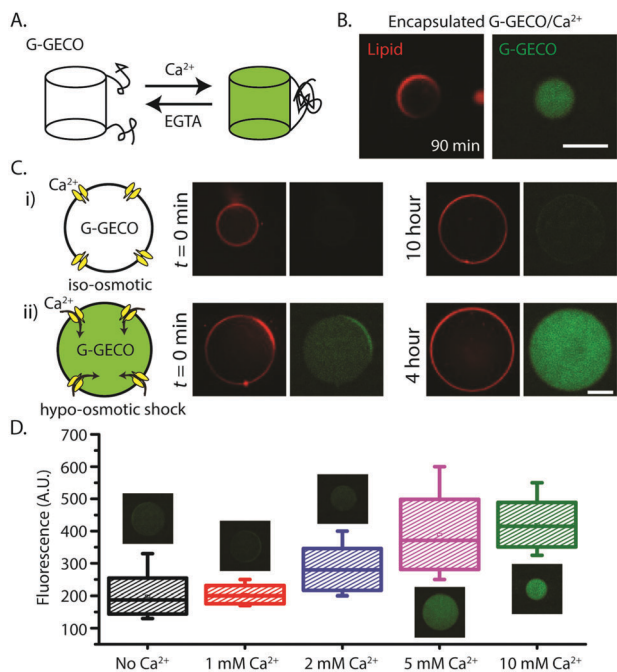


Fig. 4 Mechanosensitive and biosensing synthetic cell system. (A) Schematic depicting the reversible transformation between the fluorescent and non-fluorescent states of G-GECO protein in presence of calcium and EGTA. (B) Fluorescence images of G-GECO expression with calcium inside vesicles (1 nM P70a-G-GECO, 1.5 mM calcium chloride) was added to TXTL reaction after 1.5 hour incubation prior to encapsulation. (C) (i and ii) Three plasmid expression under different external conditions. Concentrations of P70a-S28, P28a-MscL and P70a-G-GECO in cell-free reaction were fixed at 0.2 nM, 1.4 nM and 0.6 nM respectively. The outer solutions for all conditions contained 10 mM calcium chloride. (D) Box plot showing the relative fluorescence intensities from vesicles in hypo-osmotic media with different external calcium concentrations. Each box corresponds to intensity values from ten vesicles. Plasmid concentrations of P70a-S28, P28a-MscL and P70a-G-GECO were 0.4 nM, 1.3 nM and 1 nM respectively. For both (C) and (D), the lipid vesicles were introduced into hypo-osmotic solution immediately after encapsulation following a 1.5 hour incubation period. EGTA was used at a concentration of 1 mM in all cell-free reactions. Imaging for (D) was carried out after 2 hour incubation in the hyposmotic medium. The osmolality difference between iso-osmotic and hypo-osmotic solutions was measured at 100 mOsm. All experiments were repeated three times under identical conditions. Scale bars: 50 μ m.

the lipid bilayer membrane through MscL (Fig. 4C(ii)). To our knowledge, this is the first demonstration of an AND-gate composed of a mechanical input (*i.e.* hypo-osmotic pressure) and an external chemical input (*i.e.* Ca²⁺) that lead to a specific fluorescence response. The synthetic cell system is also sensitive to the concentration of calcium added to the external solution (Fig. 4D and Fig. S6, ESI[†]). The detection time for calcium intake was as short as 20 minutes.

In summary, we have generated a DNA-programmed cell-sized artificial cell that senses osmotic pressure and external calcium concentration. We demonstrated two different circuit architectures for TXTL that exhibit different reaction kinetics that are preserved across length scale from bulk reactions to micron-sized encapsulated droplets or vesicles. The ability to endow artificial cells with mechanosensitive functions to sense external small molecules using

genetically-encoded biosensors allows for rapid sensing, rather than relying on fluorescence reporter synthesis using chemical inducers that most studies have used.^{25,26} Recapitulating TXTL for synthetic cell engineering can be used for reconstituting cellular processes and functions.²⁷ It can also serve as a powerful platform for chemical applications, such as biosensing and novel synthetic pathways for chemicals.

We thank Takanari Inoue (Johns Hopkins University) for providing the G-GECO plasmid. This work is supported by the NSF MCB-1612917 to A. P. L. and MCB-1613677 to V. N., the NIH Director's New Innovator Award DP2 HL117748-01 to A. P. L., and the Human Frontier Science Program grant number RGP0037/2015 to V. N. Y.-L. W. acknowledges support from the Global Networking Talent 3.0 Plan by Medical Device Innovation Center, NCKU. M. D. is supported by a NSF graduate fellowship.

Notes and references

- 1 E. D. Carlson, R. Gan, C. E. Hodgman and M. C. Jewett, *Biotechnol. Adv.*, 2012, **30**, 1185–1194.
- 2 J. Garamella, R. Marshall, M. Rustad and V. Noireaux, *ACS Synth. Biol.*, 2016, **5**, 344–355.
- 3 Y. Iwane, A. Hitomi, H. Murakami, T. Katoh, Y. Goto and H. Suga, *Nat. Chem.*, 2016, **8**, 317–325.
- 4 A. M. Tayar, E. Karzbrun, V. Noireaux and R. H. Bar-Ziv, *Nat. Phys.*, 2015, **11**, 1037–1041.
- 5 K. Pardee, S. Slomovic, P. Q. Nguyen, J. W. Lee, N. Donghia, D. Burrill, T. Ferrante, F. R. McSorley, Y. Furuta, A. Vernet, M. Lewandowski, C. N. Boddy, N. S. Joshi and J. J. Collins, *Cell*, 2016, **167**, 248–259, e212.
- 6 P. P. Ng, M. Jia, K. G. Patel, J. D. Brody, J. R. Swartz, S. Levy and R. Levy, *Proc. Natl. Acad. Sci. U. S. A.*, 2012, **109**, 14526–14531.
- 7 Y. Chemla, E. Ozer, O. Schlesinger, V. Noireaux and L. Alfonta, *Biotechnol. Bioeng.*, 2015, **112**, 1663–1672.
- 8 S. H. Hong, Y. C. Kwon and M. C. Jewett, *Front. Chem.*, 2014, **2**, 34.
- 9 M. K. Takahashi, C. A. Hayes, J. Chappell, Z. Z. Sun, R. M. Murray, V. Noireaux and J. B. Lucks, *Methods*, 2015, **86**, 60–72.
- 10 F. Caschera, J. W. Lee, K. K. Ho, A. P. Liu and M. C. Jewett, *Chem. Commun.*, 2016, **52**, 5467–5469.
- 11 V. Noireaux and A. Libchaber, *Proc. Natl. Acad. Sci. U. S. A.*, 2004, **101**, 17669–17674.
- 12 E. Karzbrun, A. M. Tayar, V. Noireaux and R. H. Bar-Ziv, *Science*, 2014, **345**, 829–832.
- 13 K. K. Ho, J. W. Lee, G. Durand, S. Majumder and A. P. Liu, *PLoS One*, 2017, **12**, e0174689.
- 14 A. Pohorille and D. Deamer, *Trends Biotechnol.*, 2002, **20**, 123–128.
- 15 S. Fujii, T. Matsuura, T. Sunami, T. Nishikawa, Y. Kazuta and T. Yomo, *Nat. Protoc.*, 2014, **9**, 1578–1591.
- 16 S. Hamada, M. Tabuchi, T. Toyota, T. Sakurai, T. Hosoi, T. Nomoto, K. Nakatani, M. Fujinami and R. Kanzaki, *Chem. Commun.*, 2014, **50**, 2958–2961.
- 17 Y. Zhao, S. Araki, J. Wu, T. Teramoto, Y. F. Chang, M. Nakano, A. S. Abdelfattah, M. Fujiwara, T. Ishihara, T. Nagai and R. E. Campbell, *Science*, 2011, **333**, 1888–1891.
- 18 C. D. Cox, C. Bae, L. Ziegler, S. Hartley, V. Nikolova-Krstevski, P. R. Rohde, C. A. Ng, F. Sachs, P. A. Gottlieb and B. Martinac, *Nat. Commun.*, 2016, **7**, 10366.
- 19 L. M. Lee and A. P. Liu, *Lab Chip*, 2015, **15**, 264–273.
- 20 J. Heureaux, D. Chen, V. L. Murray, C. X. Deng and A. P. Liu, *Cell. Mol. Bioeng.*, 2014, **7**, 307–319.
- 21 S. Su, S. C. Phua, R. DeRose, S. Chiba, K. Narita, P. N. Kalugin, T. Katada, K. Kontani, S. Takeda and T. Inoue, *Nat. Methods*, 2013, **10**, 1105–1107.
- 22 K. K. Ho, V. L. Murray and A. P. Liu, *Methods Cell Biol.*, 2015, **128**, 303–318.
- 23 A. S. Utada, E. Lorenceau, D. R. Link, P. D. Kaplan, H. A. Stone and D. A. Weitz, *Science*, 2005, **308**, 537–541.
- 24 K. K. Ho, L. M. Lee and A. P. Liu, *Sci. Rep.*, 2016, **6**, 32912.
- 25 J. Shin and V. Noireaux, *ACS Synth. Biol.*, 2012, **1**, 29–41.
- 26 P. Siuti, J. Yazbek and T. K. Lu, *Nat. Biotechnol.*, 2013, **31**, 448–452.
- 27 A. P. Liu and D. A. Fletcher, *Nat. Rev. Mol. Cell Biol.*, 2009, **10**, 644–650.

Supplementary information for:

Cell-sized mechanosensitive and biosensing compartment programmed with DNA

Sagardip Majumder^{1,†}, Jonathan Garamella^{2,†}, Ying-Lin Wang³, Maxwell DeNies⁴, Vincent Noireaux^{2,*}, Allen P. Liu^{1,4,5,6*}

¹ Department of Mechanical Engineering, University of Michigan, Ann Arbor, Michigan, United States

² School of Physics and Astronomy, University of Minnesota, Minneapolis, Minnesota, United States

³ Department of Biomedical Engineering, National Cheng Kung University, Tainan, Taiwan

⁴ Cellular and Molecular Biology Program, University of Michigan, Ann Arbor, Michigan, United States

⁵ Department of Biomedical Engineering, University of Michigan, Ann Arbor, Michigan, United States

⁶ Biophysics Program, University of Michigan, Ann Arbor, Michigan, United States.

† S.M. and J.G. contributed equally to this work.

* Corresponding authors: Vincent Noireaux, Ph.D., +1-612-624-6589, noireaux@umn.edu; Allen Liu, +1-734-764-7719, Ph.D., allenliu@umich.edu

Materials and Methods:

DNA constructions. The plasmids P70a-deGFP, P70a-S28, and P28a-deGFP have been described previously¹. P28a-MscL and P28a-MscL-eGFP were obtained by first cloning MscL from *E. coli* K12 into a P28a backbone and then adding eGFP as a fusion protein. The pcDNA3-G-GECO construct was obtained from Takanari Inoue (Johns Hopkins University) and the calcium-sensing function was verified by monitoring G-GECO activity from external calcium flux through ionophore A23187 (Sigma Aldrich). G-GECO was then cloned into the pT7-CFE backbone for use in a mammalian cell-free expression system. Specifically, G-GECO was PCR amplified from the pcDNA backbone and a 5' Kozak sequence and 3' CAAX sequence (in frame) added. The resulting PCR amplicon was cloned into the pT7-CFE empty vector between the plasmid IRES and poly-A tail sequence using BamHI and NotI. pT7-G-GECO DNA sequence was confirmed by sanger sequencing and its function was verified in bulk mammalian cell-free expression assays with and without calcium. Subsequently, restriction enzyme cloning from the pT7 construct into P70a-deGFP was carried out to obtain the P70a-G-GECO plasmid used in the present study. Due to lack of appropriate restriction cut sites, the gene for G-GECO was PCR amplified along with the 3' CAAX motif, and inserted by restriction enzyme cloning using PspXI and NcoI, in between the ribosome binding site and the T500 terminator sequences of the P70a-deGFP vector.

TXTL preparation and reactions. TXTL reactions are composed of the *E. coli* lysate, an amino acid mixture, and an energy buffer. Transcription and translation are performed by the endogenous molecular components provided by the *E. coli* cytoplasmic extract. A detailed description of the standard TXTL preparation has been reported previously in several articles¹⁻³. The energy buffer is composed of: 50 mM HEPES pH 8, 1.5 mM ATP and GTP, 0.9 mM CTP and UTP, 0.2 mg/ml tRNA, 0.26 mM coenzyme A, 0.33 mM NAD, 0.75 mM cAMP, 0.068 mM folinic acid, 1 mM spermidine, 30 mM 3-PGA, 2% PEG8000, either 10-15 mM maltose or 20-40 mM maltodextrin. A typical cell-free reaction is composed of 33% (volume) of *E. coli* crude extract. The other 66% of the reaction volume are composed of the energy mixture, the amino acids and plasmids. The amino acid concentration was adjusted between 1.5 mM and 3 mM of each of the 20 amino acids (always equimolar for the 20 amino acids). Mg-glutamate and K-glutamate concentrations were adjusted according to the plasmids used (typically 90 mM K-glutamate and 4 mM Mg-glutamate for P70a-deGFP). Cell-free TXTL reactions were carried out in a volume of 5 μ l to 20 μ l at 29-30°C.

Measurement of TXTL gene expression in bulk reactions. Quantitative measurements were carried out with the reporter protein deGFP (25.4 kDa, 1 mg/ml = 39.37 μ M). deGFP is a variant of the reporter eGFP that is more translatable in cell-free systems. The excitation and emission spectra as well as fluorescence properties of deGFP and eGFP are identical, as previously reported¹. The fluorescence of deGFP produced in batch mode reactions was measured on an H1m plate reader (Biotek Instruments, V-bottom 96-well plate, interval of three minutes, Ex/Em 488/525 nm). End-point measurements were carried out after 8-12 h of incubation. Pure recombinant eGFP (from either Cell Biolabs Inc. or purified in the lab) was used to make a linear calibration of intensity versus eGFP concentration for quantification on plate readers. Error bars are the standard deviations from at least three repeats. The measurements in batch more reactions for G-GECO were similar to deGFP. Measurements were recorded with a Synergy H1 plate reader (Biotek Instruments) in 96 V-bottom Nunc polypropylene plates. The temperature was set at 29°C for all conditions and kinetic measurements were carried out with an interval of

one minute. The excitation and emission wavelengths were set at 488 nm and 525 nm respectively. The measurement run was stopped at a given time and restarted after externally adding calcium to the bulk reaction. This led to a delay of 1-2 minutes indicating the loss of at most two data points at the instant of calcium addition in the supplementary figures.

Liposome preparation. Liposomes were prepared using the water-in-oil emulsion transfer method. Lipids (Egg PC, Avanti Polar Lipids) were dissolved in mineral oil (Sigma-Aldrich) at 2 mg/ml. 2-8 μ l reactions were added to 500 μ l oil and vortexed to create an emulsion. This emulsion was added atop 10-20 μ l of a feeding solution. The biphasic solution was centrifuged for 10 minutes at 1500 g to form liposomes. Single emulsion droplets were created by vortexing 6 μ l of TXTL reaction in 30 μ l of 2% Span 80 surfactant in mineral oil. Double emulsion templated vesicles were generated by a glass capillary device as described in previous works^{4,5}. DOPC, cholesterol and Liss-Rhod PE (Avanti Polar Lipids) were mixed in a glass test tube and Argon gas was used to remove the solvent. The lipids were then placed in a dessicator for an hour following which they were resuspended in a 36:64 chloroform-hexane solution by volume. The final concentration of the lipids was kept constant at 6 mg/ml for all experiments when using this device. The inner solution was prepared by adding 1.5% polyvinyl alcohol (PVA) and 1 mM EGTA (final concentrations) to a standard TXTL cell-free reaction. The cell-free solution was then incubated at 29C for an hour before encapsulation. Outer solution composition was 20 mM K-HEPES, 80 mM KCl, 1.3% glycerol, 10% PVA, and 280 mM glucose (final osmolarity is 770 mOsm). The outer solution osmolarity was matched with the inner phase by adding appropriate concentration of glucose just before encapsulation. 10 mM CaCl_2 (final conc.) was added to this outer solution for resuspending the collected double emulsions. 50 μ l of double emulsion collection was then added to 100 μ l of the outer solution containing calcium for all experimental conditions except the hypo-osmotic shock with two plasmids, in which case 50 μ l double emulsions was added to 100 μ l of the hypo-osmotic solution. The hypo-osmotic solution composition was 20 mM K-HEPES, 80 mM KCl, 10% PVA, 400 mM glucose and 10 mM CaCl_2 (final osmolarity is 660mOsm). All osmolarities were measured on a Vapro-Osmometer (by vapor pressure) with 10 μ l of sample. Following resuspension in calcium-containing solutions, the double emulsions were incubated on a slide. Oil dewetting and lipid bilayer formation was observed within a short duration after double emulsion generation.

Measurement of TXTL gene expression in liposomes. The phospholipid vesicles were observed using an inverted microscope (Olympus, IX-81) equipped with Metamorph Advanced software. Liposomes expressing deGFP/eGFP were imaged with a GFP filter set (excitation 473 nm, emission 520 nm). To image the TRITC-dextran dye (Sigma-Aldrich) and BSA-TRITC dye (Sigma-Aldrich), a Texas Red filter set was used (excitation 556 nm, emission 617 nm). At least 40 lipid vesicles were monitored to generate the standard deviation shown in the error bars. The method used to quantify the deGFP protein expression has been described previously¹. deGFP was expressed and quantified using the Biotek H1m plate reader. Then, deGFP protein at different, known concentrations was encapsulated in liposomes and standard curves of area vs intensity were created. By comparing the leading coefficients of these curves, we verify the scaling is linear. The CCD camera used was also verified to scale linearly with varying exposure times. The double emulsion templated vesicles were imaged with Olympus IX-81 spinning disk confocal microscope connected to an Andor iXOn 3 CCD camera, and operated with the Metamorph Advanced software. G-GECO and deGFP images were captured with a GFP filter set (excitation 488 nm, emission 525 nm) under constant exposure of 500 ms for all experimental conditions. A TRITC filter set (excitation 560 nm/emission 607 nm) was used to capture the fluorescent lipid images. The exposure was kept constant at 100 ms for lipid

imaging. All images were background subtracted and their contrasts were matched for visual comparison. For the quantitative analysis of calcium detection under different concentrations, integrated density (ID) measurement was carried out in ImageJ. For each image, a box was drawn based on the size of a vesicle and the ID was calculated three times by shifting the box within the lumen of the vesicle. Next, using the same box, the background ID was calculated at three different positions in the image. The relative fluorescence intensity was then calculated by subtracting the average background ID from the average luminal ID and normalizing the result with the area of the box.

References

1. J. Garamella, R. Marshall, M. Rustad and V. Noireaux, *ACS Synth Biol*, 2016, **5**, 344-355.
2. F. Caschera and V. Noireaux, *Biochimie*, 2014, **99**, 162-168.
3. Z. Z. Sun, C. A. Hayes, J. Shin, F. Caschera, R. M. Murray and V. Noireaux, *J Vis Exp*, 2013, DOI: 10.3791/50762, e50762.
4. K. K. Ho, V. L. Murray and A. P. Liu, *Methods Cell Biol*, 2015, **128**, 303-318.
5. L. R. Arriaga, S. S. Datta, S. H. Kim, E. Amstad, T. E. Kodger, F. Monroy and D. A. Weitz, *Small*, 2014, **10**, 950-956.

Supplemental Figures:

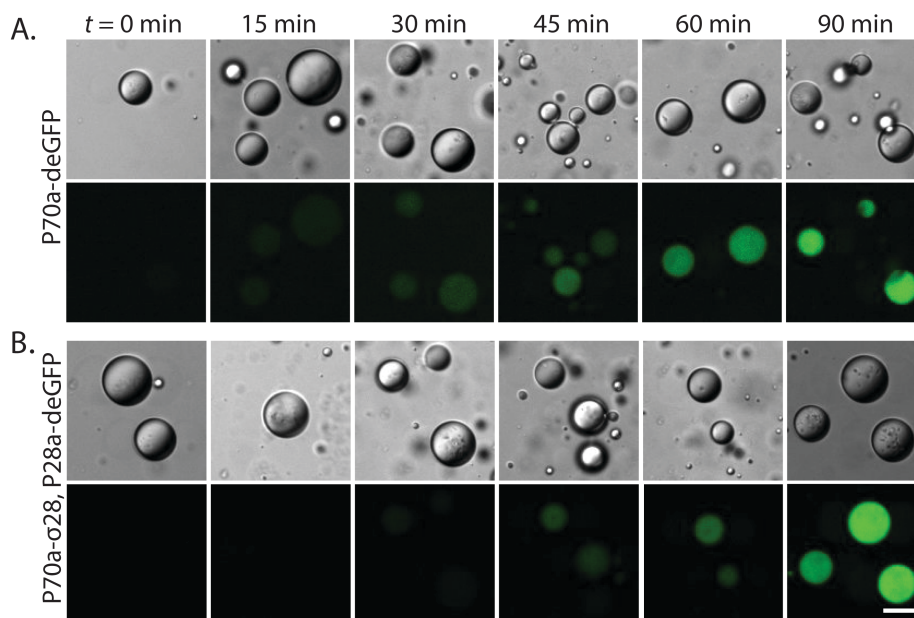


Figure S1. Encapsulation of TXTL reactions in single emulsions. (A) P70a-deGFP plasmid was used at 5nM final concentration. (B) The concentrations of P70a-S28 and P28a-deGFP were 0.2nM and 5nM respectively. Images represent a qualitative trend observed over 4-5 regions in the sample. Scale bar: 50 μ m.

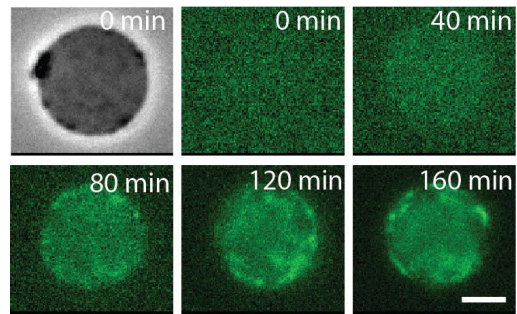


Figure S2. Synthesis of MscL-eGFP in liposomes (0.2 nM P70a-S28, 5 nM P28a-MscL-eGFP). Bright-field and fluorescence images shown at $t = 0$ min. Images taken at 40-minute interval with GFP channel. Scale bar: 5 μ m.

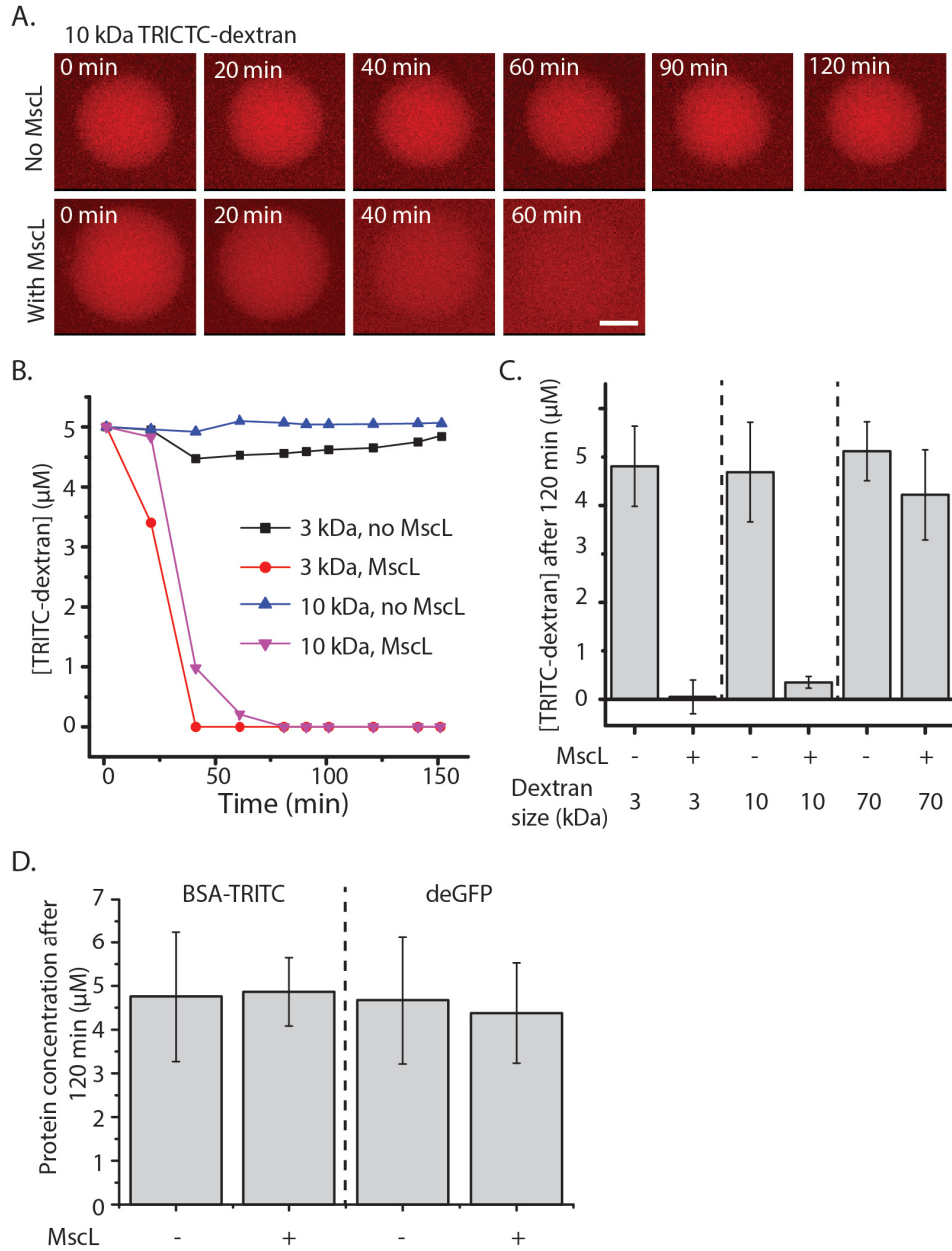


Figure S3. Leakage of TRITC-dextran of varying sizes in liposomes in the absence or presence of MscL. (A) Top: Fluorescence images of liposomes containing 10 kDa TRITC-dextran over a 2-hour period without P28a-MscL in the TXTL reaction. Bottom: Fluorescence images of liposomes containing 5 μ M 10 kDa TRITC-dextran over a 60-minute period with P28a-MscL the TXTL reaction. Scale bar: 5 μ m. (B) Liposome kinetics of 3 and 10 kDa TRITC-dextran concentration in the presence or absence of MscL. (C) Bar graph of average TRITC-dextran concentration at 0 and 120 minutes. 5 μ M TRITC-dextran encapsulated in liposomes at $t = 0$. Sizes of dextran are 3, 10, and 70 kDa. - or + denote the absence or presence of MscL. Error bars shown are one standard deviation in each direction. Sample standard deviation is

generated from the observation of 49, 51, 45, 43, 42, and 45 liposomes for 3-, 3+, 10-, 10+, 70-, and 70+, respectively (3- indicates 5 μ M 3 kDa dextran and no MscL, 3+ indicates 5 μ M 3 kDa and 5 nM MscL plasmid, etc.) (D) Bar graph of average BSA-TRITC and deGFP concentration at 0 and 120 minutes. 5 μ M BSA-TRITC or deGFP encapsulated in liposomes at $t = 0$. - or + denote the absence or presence of MscL. Error bars shown are one standard deviation in each direction. Sample standard deviation is generated from the observation of 41, 41, 42, and 45 liposomes for BSA-, BSA+, deGFP-, and deGFP+, respectively (BSA- indicates 5 μ M BSA-TRITC and no MscL, BSA+ indicates 5 μ M BSA-TRITC and 5 nM MscL plasmid, etc.)

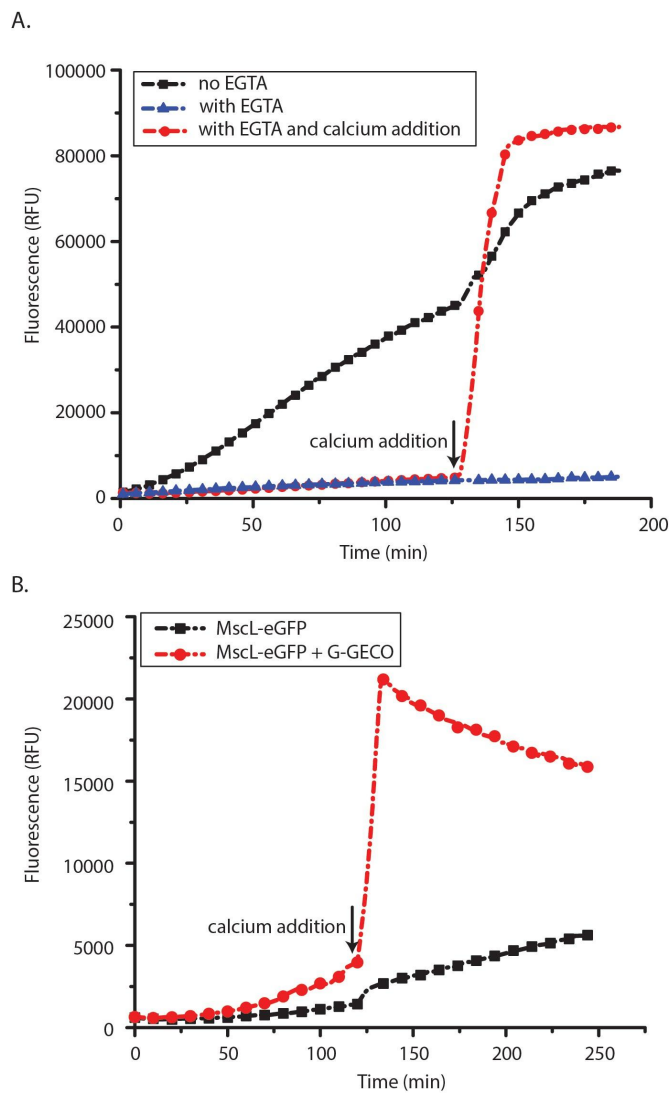


Figure S4. Expression kinetics of G-GECO in TXTL with and without calcium using P70a-G-GECO. (A) Calcium sensing by G-GECO in presence of 1 mM EGTA. 2 mM calcium chloride (final concentration) was added to bulk reaction at $t = 125$ min. Concentration of P70a-G-GECO plasmid was fixed at 1 nM for all cases. (B) Two-plasmid expression in bulk reaction. P70a-G-GECO, P70a-S28 and P28a-MscL-eGFP were added at final concentrations of 0.2 nM, 0.2 nM and 1 nM respectively. 1 mM calcium chloride was added after 120 minutes. TXTL reactions for both conditions contained 1 mM EGTA.

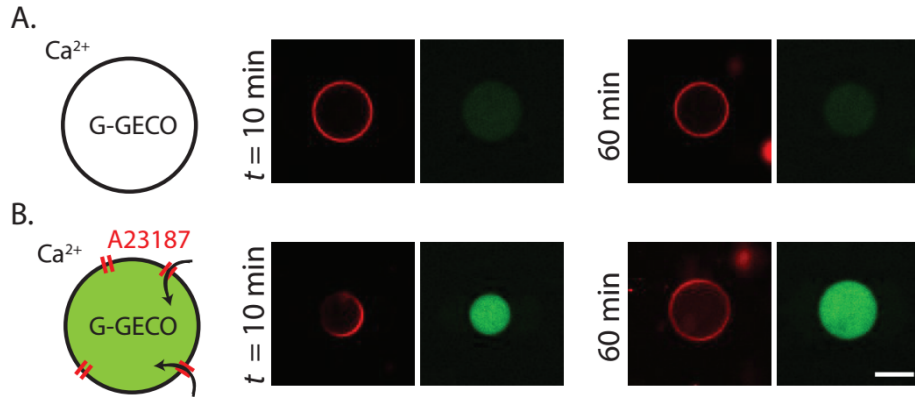


Figure S5. Calcium dependent increase in G-GECO fluorescence inside lipid vesicles. (A) Images showing the native fluorescence of cell-free expressed G-GECO after 3 hours incubation. (B) Increase in fluorescence as observed upon addition of 1 μ M A23187 (Calcium ionophore). The time points indicate incubation of vesicles after the addition of A23187 and the simultaneous control experiment without the ionophore. All cell-free reactions contained 1 mM EGTA. The calcium concentration in the outer solution was 10 mM. P70a-G-GECO plasmid was added at a concentration of 1.5 nM. Scale bar: 50 μ m.

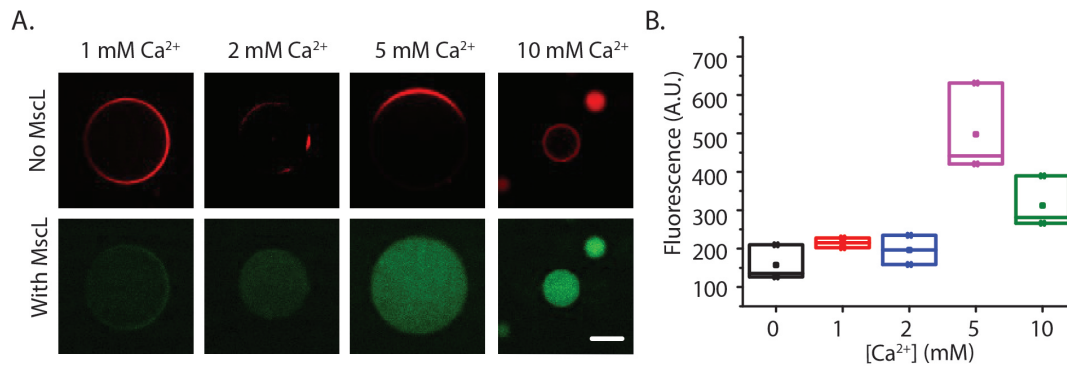


Figure S6. Osmotic downshock experiments of TXTL encapsulated vesicles (MscL and G-GECO) with different external calcium concentrations. (A) Fluorescence images of vesicles after 20 minutes of incubation following addition of hyposmotic media, for four different calcium concentrations. In contrast with the experimental condition in Figure 4, the vesicles were incubated for an hour after their generation, in isosmotic solution with no calcium, to allow for possible MscL incorporation into the lipid bilayer before the hyposmotic shock. (B) Box plot of the relative fluorescence intensities of vesicles from (A) at the same time point. The fluctuations in the relative intensities correspond to the values from six vesicles in each case. The plasmid concentrations for P70a-G-GECO, P70a-S28 and P28a-MscL were 1 nM, 0.4 nM, and 1.3 nM, respectively. EGTA was added at a concentration of 1 mM. Scale bar: 20 μ m.